Chitosan-Dextran Sulfate Hydrogels as a Potential Carrier for Probiotics

Cigdem Yucel Falco[a], Peter Falkman[b], Jens Risbo[a,], Marité Cárdenas[b], Bruno Medronho[c,*]*

[a]University of Copenhagen, Department of Food Science, Rolighedsvej 30, DK-1958, Copenhagen, Denmark.

[b]Malmö University, Biomedical Laboratory Science and Biofilm Research Center for Biointerfaces, Faculty of Health and Society, SE-205 06 Malmö, Sweden.

[c]University of Algarve, Faculty of Sciences and Technology (MeditBio), Campus de Gambelas, Ed. 8, 8005-139 Faro, Portugal.

* Corresponding authors:

Electronic mail: bfmedronho@ualg.pt (B. Medronho) and jri@food.ku.dk (J. Risbo).

ABSTRACT

Physical and chemical (crosslinked with genipin) hydrogels based on chitosan and dextran sulfate were developed and characterized as novel bio-materials suitable for probiotic encapsulation. The swelling of the hydrogels was dependent on the composition and weakly influenced by the pH of the media. The morphology analysis supports the swelling data showing distinct changes in microstructure depending on the composition. The viability and culturability tests showed approx. 3.6 log CFU/mL decrease of cells (*L. acidophilus* as model) incorporated into chemical hydrogels when compared to the number of viable native cells. However, the live/dead viability assay evidenced that a considerable amount of viable cells were still

entrapped in the hydrogel network and therefore the viability is most likely underestimated. Overall, the developed systems are robust and their structure, rheology and swelling properties can be tuned by changing the blend ratio, thus constituting appealing bio-matrices for cell encapsulation.

Keywords: Chitosan; dextran sulfate; genipin; hydrogel; encapsulation; probiotic bacteria.

1 Introduction

Hydrogels are typically defined as tridimensional polymer networks that can take up considerable amounts of solvent without dissolving due to its inherent hydrophilicity (Bhattarai, Gunn, & Zhang, 2010). Hydrogels can be used to form different physical structures such as microparticles or nanoparticles, and coatings (Hoare & Kohane, 2008). They are often highly deformable, mainly due to their unique structural tunability. Their porous structure and, consequently, swelling performance can be altered by varying the crosslinking density within the gel matrix (Hoare & Kohane, 2008). Moreover, these systems can respond to external stimuli, such as pH, light, electric field, and thus change volume and shape (Shang, Shao, & Chen, 2008). Hydrogels are therefore suitable for a broad range of applications such as drug delivery (Gupta, Vermani, & Garg, 2002; Saboktakin, Tabatabaie, Maharramov, & Ramazanov, 2010), tissue engineering (Drury & Mooney, 2003; Lee & Mooney, 2001), biomedicine (Berger, Reist, Mayer, Felt, & Gurny, 2004; Shang et al., 2008), and encapsulation technologies (Altunbas, Lee, Rajasekaran, Schneider, & Pochan, 2011; Karoubi, Ormiston, Stewart, & Courtman, 2009).

Currently, there is an increasing need for replacing synthetic hydrogel based products by natural counterparts prepared with sustainable materials from renewable resources mainly due to stricter international regulations. In this context, chitosan (CH) emerges as a popular cationic biopolymer for the formulation of colloidal hydrogels. CH is a random linear copolymer of (1-4)-N-acetyl-D-glucosamine and (1-4)-D-glucosamine units, produced by the deacetylation of the naturally occurring chitin under high alkaline conditions (Vårum & Smidsrød, 2005). Its polycationic feature is due to amine residues that are protonated

below pH ca. 6.5 (Illum & Davis, 2005). Moreover, CH is biocompatible, non-toxic (Ravi Kumar, 2000), and biodegradable (i.e. it can be metabolized by enzymes, such as lysozyme, present in human body fluids) (Prabaharan & Mano, 2005) and potentially by bacterial enzymes in the colon (Kean & Thanou, 2010). On the other hand, dextran sulfate (DXS) is one of the most studied anionic, biocompatible, and biodegradable biopolymers. It is a branched polysaccharide with 1–6 and 1–4 glycosidic linkage and contains approximately 16-19 % sulfur, which is equivalent to approximately 1.6 - 2.4 sulfate groups per glucosyl unit (Anitha et al., 2011). It is widely used in food, materials and pharmaceutical areas. Hence, DXS and CH are promising candidates for the encapsulation of different cargo due to their safety and bio-profiles. Apart from the physical systems, CH can be chemically crosslinked with remarkable impact on the rheological and physicochemical properties of formed hydrogels (Delmar & Bianco-Peled, 2015; Dimida et al., 2015). The formation of permanent covalent bonding between the biopolymer chains also improves the mechanical properties in comparison to the related physical hydrogels. In particular, genipin (GP, isolated from the gardenia plant) is an ideal crosslinker agent due to its biocompatibility and considerably lower toxic profile than glutaraldehyde, formaldehyde or other often used crosslinker agents (Bhattarai et al., 2010; Dimida et al., 2015). GP can react with the primary amine group of CH to create stiffer and stronger hydrogel network (Bhattarai et al., 2010). In addition, geniposide, abundant in some fruits, was reported to be transformed to GP in the gastrointestinal tract without an adverse effect (Butler, Ng, & Pudney, 2003).

Although the formation of physical CH-DXS hydrogels was reported earlier (Delair, 2011), we further explored the formation of GP-crosslinked CH-DXS based hydrogels with focus not only on their preparation and characterization, but also on their performance to entrap probiotic cells. Crosslinking can contribute to improve both the mechanical and pH stability of the hydrogel matrix during the harsh gastric passage. Ultimately, the goal is to produce a responsive biomaterial delivery system for probiotic bacteria that ensures a safe passage through the harsh conditions found in the stomach while allowing the release of the encapsulated content at the human colon. As a proof of concept, model probiotic bacteria, *Lactobacillus*

acidophilus, was chosen to be incorporated into the physical and chemical hydrogels whereupon their viability was assessed.

2 Materials and methods

2.1 Materials and chemicals

CH (extracted and/or purified from *Pandalus borealis* shell, low molecular weight, deacetylation ≥ 75 %), acetic acid (glacial, ≥ 99.85 %), sodium chloride (NaCl, Fluka) and potassium dihydrogen phosphate (KH_2PO_4) were purchased from Sigma-Aldrich, Steinheim, Germany. DXS (from molecular weight 500 kDa, ultra-pure grade) was obtained from Amresco, Ohio, USA. The most relevant properties of the biopolymers used are summarized in Table S1 in supporting information, SI. GP was bought from Challenge Bioproducts, Taiwan. Disodium hydrogen phosphate dihydrate (Na_2HPO_4) and potassium chloride (KCl) were obtained from Merck, Darmstadt, Germany. *Lactobacillus acidophilus* (LA5) was a kind gift from Chr. Hansen A/S, Copenhagen, Denmark. MRS broth (de Man, Rogosa and Sharpe), MRS agar, and atmosphere generation system (AnaeroGen sachets) were bought from Oxoid, Basingstoke, England. The MRS agar and broth were sterilized in an autoclave (115 °C, 10 min). The live/dead® BacLight™ bacterial viability kit for microscopy was bought from ThermoFisher Scientific, Molecular Probes, Eugene, OR, USA. All the chemicals were used as received. Milli-Q water (18.2 MΩ·cm at 25 °C) was used in all experiments.

2.2 Preparation of the biopolymer solutions

Concentrated CH stock solutions (2, 3, and 4 wt %) were prepared by dissolving a known amount of CH into 1 % v/v glacial acetic acid. The solutions were stirred with a magnetic stirrer for at least 12 h until a clear solution was obtained. The DXS stock solutions (2 and 3 wt %) were simply prepared in Milli-Q water. Depending on the solution, all the necessary dilutions were made either with 1 % v/v glacial acetic acid or Milli-Q water without pH adjustment. The pH of 3 wt % CH was approx. 4.8, while it was approx. 7.0 for the 2 wt % DXS.

2.3 Preparation of physical and chemical hydrogels

After the preparation of the pure biopolymer solutions, several samples were prepared by adding equal volume of the CH aqueous solution (typically 2.5 mL) into the DXS aqueous solution (typically 2.5 mL). The samples were stirred at room temperature until a homogeneous mixture was obtained (approx. 19-24 h). The hydrogel samples were visually checked (naked eye) for several days. To form the chemical hydrogels, GP stock solutions (0.5 and 1 wt %) were prepared in Milli-Q water and diluted when necessary. The most promising CH and DXS blend ratios were chosen to be crosslinked with different amounts of GP (from 0.05 to 0.3 wt % in the final mixture). Note that the GP solution was added to the DXS solution prior to adding the CH solution. The final mixtures were stirred for 19 to 24 h at room temperature until homogeneous gels were obtained. The compositions of hydrogels given in the following text refer to the component amount in the final mixtures. The pH of final mixtures was between 4.7 – 4.9 (well below the pKa of CH, approx. 6.5) and therefore CH is expected to have a reasonably high charge density.

2.4 Bead formation

Apart from the bulky hydrogels, the formation of beads was explored by dropwise addition of different concentrations of the CH aqueous solutions (using a 200 µL pipette tip) into different DXS solutions and vice versa. For the formation of the chemical crosslinked beads, the CH solution was dripped into DXS solution in which an appropriate amount of GP was previously mixed. The beads were left to cure at room temperature for 12 h.

2.5 Rheological characterization

The rheological properties of physical and chemical hydrogels were measured at 25 °C using Haake Mars III rheometer (Thermo Scientific, Karlsruhe, Germany) equipped with a cone and plate measuring geometry (1° cone angle, 35 mm diameter, and 0.05 mm gap). For the steady state viscosity measurements, the shear rate was linearly increased from 0.01 to 100 s^{-1}. For the dynamic viscoelastic measurements, the linear viscoelastic regime was initially determined via stress sweep experiments (0.1 to 50 Pa) at constant

frequency (1 Hz). Frequency sweep test (from 10 to 0.01 Hz) was then conducted by applying a constant stress within the linear region (typically, 1 and 4 Pa for the physical and chemical hydrogels, respectively). The dynamic mechanical spectra were obtained recording the storage modulus (G') and loss modulus (G") as a function of frequency.

2.6 Swelling experiments

The different physical and chemical hydrogels were tested regarding their swelling profile in aqueous solutions at pH 2.0 (0.1 M HCl) and pH 7.4 (0.1 M NaOH). The systems tested comprised hydrogels where the CH and GP concentrations were kept constant (1.5 and 0.1 wt %, respectively) while the DXS concentration was varied (i.e. 0, 1, and 1.25 wt %). Alternatively, CH and DXS concentrations were kept constant at 1.5 and 1 wt %, respectively, while the GP concentration was varied (i.e. 0, 0.1, and 0.15 wt %). Prior to the swelling experiments, the hydrogels were left to cure for a similar period (approx. 27-29 h). The swelling experiments were performed following an adapted method previously reported (Delmar & Bianco-Peled, 2015). In brief, the hydrogels (in triplicates, approx. 50-60 mg) were submerged in Eppendorf tubes containing 1.5 mL of aqueous solution at either pH 2.0 or 7.4. The tests were performed using a series of Eppendorf tubes, one for each sampling point (ie. 1, 2, 3, 4, 5, 10, 20, 30 min). Water evaporation was minimized by closing the Eppendorf lids during the experiment. Each gel was weighed periodically after removing the swelling media from the tubes. The swelling percentage, *Q %*, was determined over time using Eq.1.

$$Q, \% = \frac{mt - m0}{m0} \times 100 \qquad (1)$$

where m_0 is the initial weight of the hydrogel and m_t is the weight of the hydrogel at time *t*. Data were expressed by the average of *Q %* values from triplicates ± standard deviation. The equilibrium swelling (Q_{eq} *%*) was estimated from the *Q %* vs. *t* curve for each type of hydrogel upon reaching steady state.

2.7 Morphological characterization by scanning electron microscopy

The morphology of the hydrogels and beads was assessed by scanning electron microscopy (SEM, Zeiss EVO LS10) equipped with a LaB6 filament operating at 15 kV and with 50 pA probe current in high vacuum mode. Sample preparation was adapted from a previous method (Wang & Chen, 2016). In brief, the hydrogel samples or beads were spread and/or fixed on carbon tape on an aluminum stub and then frozen (in a freezer) at -80 °C for 2 h. The samples were then lyophilized in two freeze drying stages: 1) at -55 °C for 1 h and 2) at 20 °C for 30 min. The second step prevents the formation of condensation when the samples are removed from the freeze dryer. Afterwards, the specimens were sputter coated with gold using an Agar automatic sputter coater, and a conductive bridge was "painted" between the sample top surface and the stub using Electrodag 1415, for those samples whose geometry prevented complete coating. ImageJ software was used to process images.

2.8 Growth of Lactobacillus acidophilus

L. acidophilus was anaerobically propagated (100 µL) from a frozen stock in 10 mL MRS broth at 37 °C, for 24 h and then 250 µL of the preculture was anaerobically incubated in 50 mL MRS broth at 37 °C, for 16 h in a glass bottle. After growth, the cells were harvested by centrifuging (4000 × g, 5 min, and 4 °C). After discarding the supernatant, the pellet was re-suspended in 0.1 M 50 mL phosphate buffered saline (PBS), pH 7.4 (8 g/L NaCl, 0.2 g/L, 1.44 g/L Na_2HPO_4, and 0.24 g/L KH_2PO_4) and centrifuged again. This washing procedure was repeated twice, and the cells were either incorporated in the hydrogels or re-suspended in 50 mL PBS, pH 7.4 for enumeration.

2.9 Incorporation of cells into hydrogels

Initially, the CH (3 wt %) and DXS (2 wt %) stock solutions were sterilized by autoclaving at 121 °C for 20 min. Before and after autoclaving the pH of the CH solution was approx. 4.8. The pH of DXS solution dropped from approx. 7.0 to 1.6 after autoclaving. However, the final pH of the mixture was approx. 4.4. The most promising hydrogel compositions were chosen for entrapment of cells, namely a physical

159 hydrogel containing 1.5 wt % CH and 1 wt % DXS, and a chemical crosslinked hydrogel containing 1.5 wt%
160 CH, 1 wt % DXS, and 0.1 wt % GP. The procedure was as follows: 5 mL of CH (3 wt %) were introduced into
161 the previously obtained washed cell pellet and vortexed briefly. 5 mL DXS (2 wt %) were added in the
162 following step and vortexed again. For the formation of GP crosslinked gels, 10 mg of GP were added
163 before incubating the gels at 37 °C and 225 rpm for 3 h.

164 ### *2.10 Viability and culturability of free and incorporated cells*

165 The viable cell count and culturability examination for free and incorporated bacteria into the hydrogels
166 was done by the spread-plate method. After 3 h of incubation in the hydrogels, 40 mL PBS, pH 7.4 was
167 added into 10 mL of the hydrogel and further homogenized in a stomacher (Seward, Stomacher 400, Lab
168 System) using proper bags with side filter for 2 min at normal speed in order to release the cells trapped in
169 the hydrogel. As a positive control, free cells were plated after being washed with PBS, pH 7.4. In the
170 spread-plate method, 0.1 ml of an appropriately diluted culture using 0.1 M PBS, pH 7.4 was spread over
171 the surface of previously prepared MRS agar plates in duplicates. The plates were then incubated
172 aerobically at 37 °C for 48 h. The viability count for the suspension of free or released cells from hydrogels
173 was expressed as colony forming units per milliliter (CFU/mL). The data are reported as the average of the
174 number of viable cells ± standard deviation from the duplicated experiments of duplicated plating.
175 Moreover, a qualitative viability assessment was carried out using the live/dead bacterial viability kit for
176 1) the cells released from physical hydrogel, and 2) the residual part of the hydrogel (containing unreleased
177 cells) in the stomacher bag after homogenization. It is essentially a two-colour fluorescence assay kit. The
178 stain was prepared and applied following manufacturer's instructions. Photomicrographs of cells were
179 acquired using Zeiss Axioskop microscope (Carl Zeiss, Goettingen, Germany) equipped with a Cool Snap RS
180 Photometrics camera (Roper Scientific, Tucson, AZ, USA) and using an appropriate fluorescence filter. The
181 images were taken with 40 x objectives and they were processed using the ImageJ software.

182 ## 3 Results and discussion

3.1 Gel formation and rheology

The gelling process was slow and continuously developed throughout the 20-24 h of gentle stirring, which indicates a slow organization of the network. Fresh hydrogels were observed to be formed only in the CH and DXS concentration region of approx. 1-2 wt % and 1-2.5 wt %, respectively. However, with time and/or centrifugation it became clear that some of the formulations initially labeled as gels were not stable and eventually phase separated. The stable hydrogels were formed when 1.5 wt % CH was mixed with 1 or 1.5 wt % DXS. In such systems, the gain in entropy upon mixing oppositely charged polyelectrolytes is due to release of the bound counterions that drives the associative phase separation (Kronberg, Holmberg, & Lindman, 2014). Hence, stable hydrogels were found to be formed at a charge density ratio (n^+/n^-) of around 0.95-1.4 (see SI for charge density calculations). It is out of the scope of this paper to investigate in detail the phase behaviour of CH and DXS mixtures, but it is suggested that the observed phase separation for some formulations might be due to the expelling excess solvent after the formation of the coacervate. The reason behind such a phenomenon (also known as syneresis) is likely the thermodynamic imbalance, which leads to the reorganization of the polymer chains within the hydrogel network and consequent exclusion of solvent (Delmar & Bianco-Peled, 2015). This is a typical consequence of associative phase separation.

The samples that were visually identified as hydrogels were further examined regarding their rheological properties. Figure 1A shows typical flow curves for mixtures of CH and DXS exhibiting a non-Newtonian shear thinning behaviour regardless of the DXS concentration. The flow curves were also reversible with a small hysteresis area when shear rate was consecutively increased and decreased (data not shown). In Figure 1B, typical oscillatory frequency sweep tests are also depicted. In all the cases, the G' was higher than the G'' and essentially frequency independent. These are the typical rheological fingerprints for gel-like materials (Picout & Ross-Murphy, 2003).

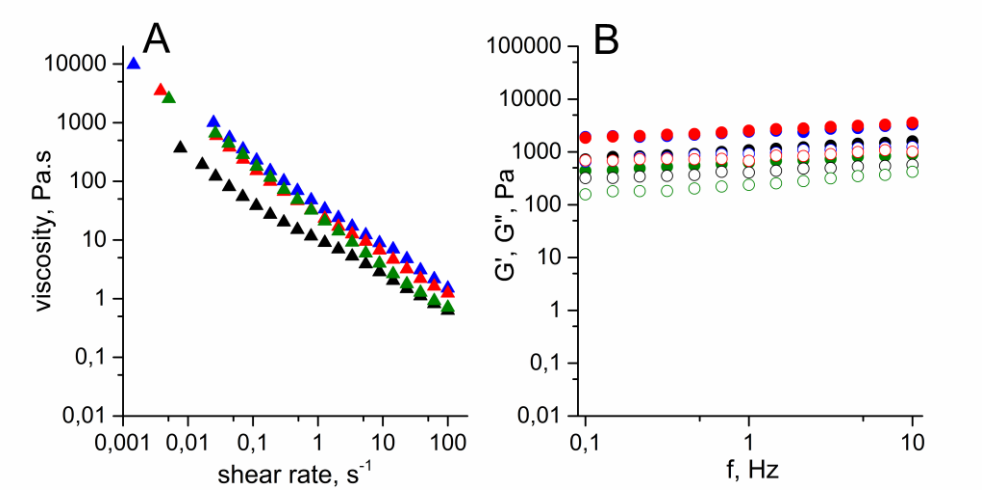

Figure 1. Rheological properties of physical hydrogels: A) typical flow curves and B) typical dynamic mechanical spectra (full symbols represent G' while empty symbols represent G'') of preparations of 1.5 wt % CH with varied DXS concentrations: 1 wt % (black), 1.5 wt % (blue), 2 wt % (red), and 2.5 wt % (green) at 25 °C.

Similar rheological profiles were observed for the other formulations and in Figure 2 the shear viscosity (at $\dot{\gamma} = 0.01\ s^{-1}$), G' and G'' at a constant frequency are reported at 25 and 37 °C. The temperature effect is clear; regardless of the CH and DXS concentrations, shear viscosity and G' were lower at 37 °C than at 25 °C and this can be considered a normal temperature effect where, in general, polymer chains in solution become more mobile with increased temperature. Another interesting feature is that both G' and shear viscosity seemed to reach a maximum at a charge density ratio close to 1. This trend was observed while keeping CH concentration constant and changing DXS concentration or vice-versa. Such an increase in the rheological properties is explained by the maximized electrostatic interactions and physical entanglements close to the 1:1 stoichiometry. However, when the entire polymer chains become neutralized, further increase of one of the polymers does not improve the 3D structure. In fact, above the 1:1 ratio, the system becomes overcharged, and polymer repulsion within the gel weakens the structure. This kind of complex

pattern was reported previously, in gels prepared with cationic cellulose derivative (cat-HEC) and double-stranded DNA (dos Santos, Piculell, Medronho, Miguel, & Lindman, 2012).

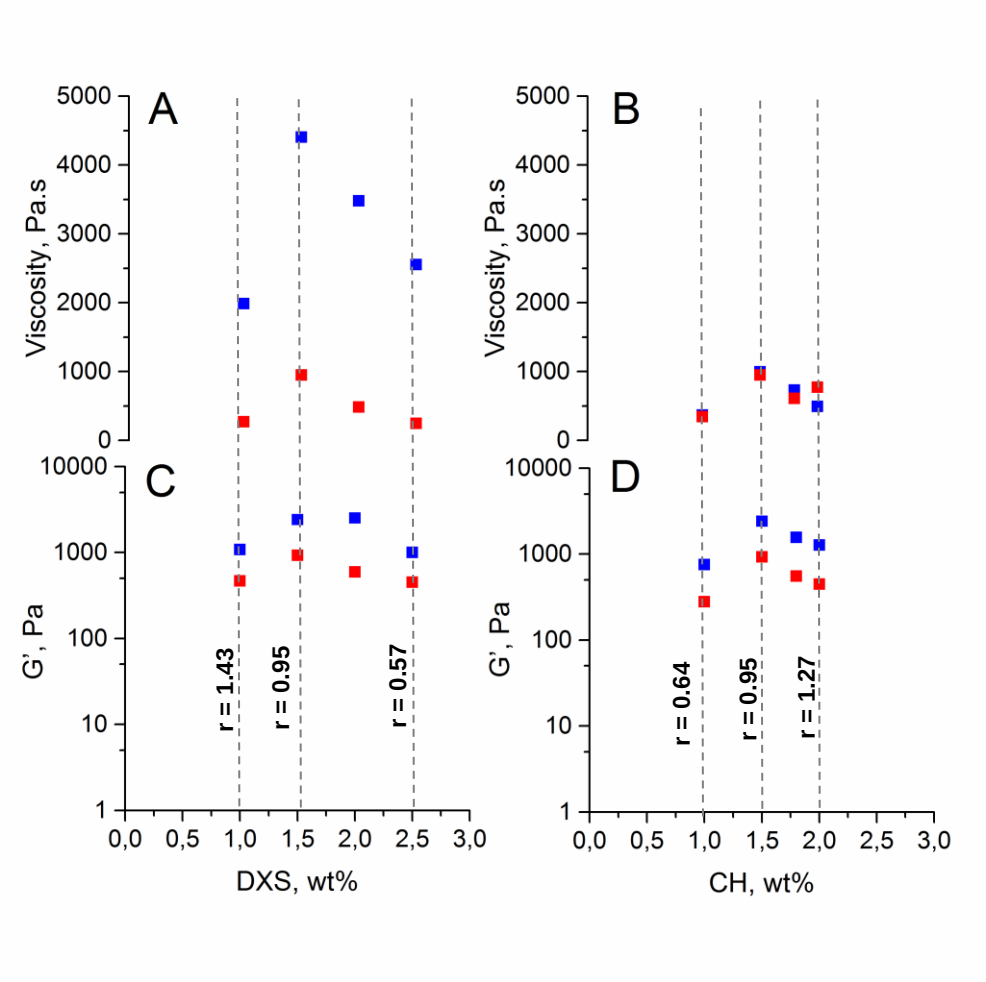

Figure 2. Shear viscosity (at $\dot{\gamma} = 0.01\ s^{-1}$) and G' (1 Hz) as a function of DXS (CH kept constant at 1.5 wt %) and CH (DXS was kept constant at 1.5 wt %) concentrations at 25 °C (red) and 37 °C (blue). The pH of mixtures was always between 4.7 - 4.9. Different charge ratios, r, are inserted as vertical dashed lines.

The most promising physical systems were selected to be crosslinked by GP with focus on the hydrogels prepared with 1.5 wt % CH and 1 wt % DXS. Typically, hydrogels crosslinked with GP exhibited a dark blue colour, which is associated with GP reaction with the amino groups of CH (Dimida et al., 2015). The rheology tests were performed on the chemically crosslinked gels after about 2-3 days of crosslinking

reaction. In such conditions, GP is expected to have reacted and therefore the system should have reached equilibrium. In Figure 3A, the chemical hydrogels showed a non-Newtonian shear thinning behaviour regardless of GP concentration. As expected, the oscillatory frequency sweep showed a typical gel-like pattern independent of GP concentration (Figure 3B).

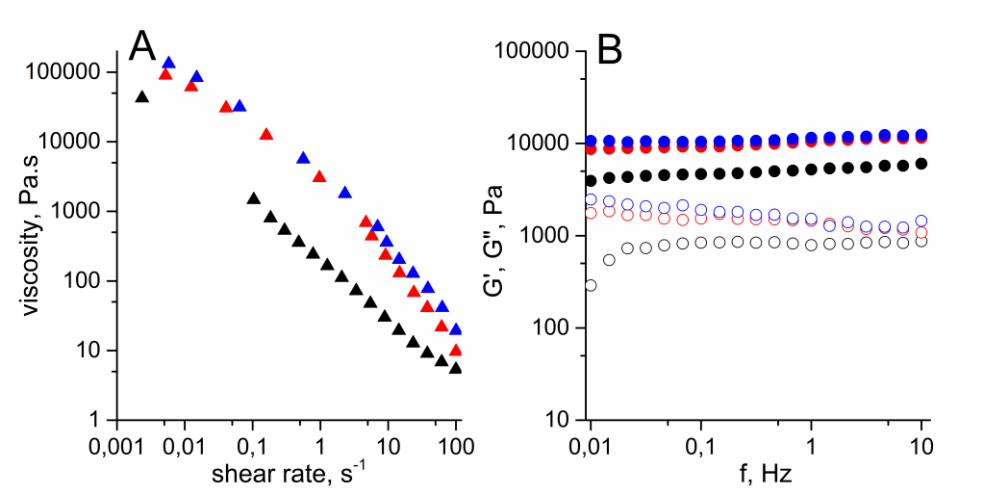

Figure 3. Rheological properties of GP crosslinked hydrogels prepared with 1.5 wt % CH and 1 wt % DXS: A) typical flow curves and B) typical dynamic mechanical spectra (full symbols represent G' while empty symbols represent G'') for GP concentrations of 0.05 (black), 0.1 (red) and 0.15 wt % (blue) at 25 °C.

Increasing the GP concentration led firstly to a pronounced increase on the viscosity and G' while no major changes were observed above 0.1 - 0.15 wt % GP (see SI, Figure S1). Linear relations between the GP content and the viscoelastic properties (i.e. G') was reported for CH chemical hydrogels (Dimida et al., 2015; Moura, Figueiredo, & Gil, 2007). The plateau observed above 0.15 wt % GP might be related to the saturation of CH with GP. The maximum in the rheological properties corresponds roughly to an estimated stoichiometry of 1:6 (i.e. one genipin crosslinked to chitosan every 6 units). Since G' does not change upon GP increase, this suggests the increase in crosslinking density is most likely hindered due to steric effects. Moreover, the role of DXS in the 3D network can contribute to a more complex behaviour as compared to

252 simple CH systems. Particularly, the shear viscosity and G' increased about approx. 2-3 times, when DXS
253 was added in the hydrogel in comparison with the systems without DXS (see SI, Table S2). Additionally, the
254 GP effect is striking; the shear viscosity increased approx. 100 times while G' was enhanced approx. 7 times
255 (see SI, Table S2). One of the requirements for an efficient material to deliver probiotic cells is its capability
256 to protect the cells from the imposed external mechanical stresses. Thus, the enhancement of the
257 mechanical resistance of the matrix improves the conditions for a safe passage of the encapsulated cells
258 through the gastrointestinal tract (Vos, Faas, Spasojevic, Sikkema, & De Vos, 2010). Overall, the chemical
259 gels are stronger and stiffer than the physical counterparts and they seem to display mechanical properties
260 highly suitable for probiotic encapsulation and delivery.

261 ### *3.2 Bead Formation*

262 So far the discussion has focused on bulk physical and chemical hydrogels. However, for several
263 applications, the encapsulation of probiotics requires small delivery systems. Therefore, it is important to
264 investigate whether the formulations screened for the bulk hydrogels can also be used to produce smaller
265 particles. Different concentrations of CH and DXS were tried in order to form beads by either dripping CH
266 into DXS or vice versa. In order to obtain physical beads, very high initial concentrations of DXS (approx. ≥
267 10 wt %) were needed (see SI, Figure S2A). On the other hand, the chemically crosslinked beads were
268 formed by dripping CH into the solution of DXS and GP (see SI, Figure S2B). Crosslinked beads were
269 successfully obtained by either dripping 2-3 wt % CH into a solution of 1-2 wt % DXS containing a fixed
270 amount of GP (0.1 wt %). The dark blue colour of the beads is indicative of a successful crosslinking and was
271 observed after allowing the reaction to run for 20 h at room temperature.

272 ### *3.3 Hydrogel swelling*

273 The swelling kinetics is an important property for different applications of hydrogels. Therefore, the
274 hydrogel composition (CH-DXS ratio) and crosslinker concentration in the hydrogel were investigated
275 regarding their effect on the swelling behaviour of the systems at low pH, 2.0 and high pH, 7.4. The swelling

isotherms are represented in Figure 4 for pH 2.0 (for pH 7.4 see SI, Figure S3). A linear behaviour was observed in all the cases regardless of pH. Moreover, Figure 5 shows the variation of the equilibrium degree of swelling as a function of DXS (0, 1, 1.25 wt %) and GP (0, 0.05, 0.1 and 0.15 wt %) concentrations. Regardless of the pH, the equilibrium swelling decreased as the DXS concentration increased in the hydrogel (Figure 5A). This might be due to the physical reinforcement of the 3D network when the DXS approaches the charge ratio of CH, which is in agreement with the rheological data in Figure 2. Upon increasing DXS concentration (up to 1.5 wt %), the hydrogel became stronger (i.e. solid-like) and showed a more restricted swelling. Similar swelling profile in acidic (pH 2.0) and basic (pH 8.0) media was previously observed for hydrogel of CH (with a DA of 18.1 %) and DXS (Sakiyama, Takata, Kikuchi, & Nakanishi, 1999). Moreover, increasing the GP concentration (from 0 to 0.15 wt %) in the gel matrix led to a decrease in the equilibrium swelling percentage regardless of the pH (Figure 5B). Similar observations were reported, for instance, for hydrogels of dimethylaminoethyl acrylate methyl chloride quaternary salt crosslinked with acrylic acid (Katime, 2010). In general, the deformation of a hydrogel becomes more restricted by increasing the crosslinker content and often this leads to a less flexible hydrogel structure. Again, such swelling behaviour performance is in good agreement with the rheological properties of the chemical hydrogels presented in Figure S1, where the G' and shear viscosity are observed to increase with the GP concentration from 0 to 0.15 wt %. Note that, the physical gel (CH/DXS) dissolved and/or considerably degraded at pH 2.0. This result indicates the importance of crosslinking of the hydrogel to be able to stand the harsh acidic conditions of the stomach.

The swelling kinetics was investigated by fitting the experimental data assuming a second order kinetics. Since the water content at different times (W, %) can be expressed by

$$W, \% = \frac{mt - m0}{mt} \times 100 \qquad (2)$$

Thus, the swelling rate at any time is expressed by (Katime, 2010; Schott, 1990)

$$\frac{dW}{dt} = K\left(W_{eq} - W\right)^2 \qquad (3)$$

where W_{eq} is the water content at the equilibrium and K is kinetics rate constant.

Rearranging Eq. 3, it can be demonstrated that the data must fit a straight line with a slope of $1/W_{eq}$ with ordinate of $1/KW_{eq}^2$. Then, the kinetics rate constant can be calculated from the following relation (Katime, 2010):

$$\frac{t}{W} = \frac{1}{KW_{eq}^2} + \frac{t}{W_{eq}} \qquad (4)$$

The experimental data were well fitted by Eq.4 with $R^2 \geq 0.99$ for all the tested hydrogels as exemplified in Figure 4C. In general, all the analyzed crosslinked hydrogels achieved the swelling equilibrium reasonably fast (i.e. during the first 5 min), except for the chemical system without DXS. This fast swelling equilibrium was also observed in other systems such as for UV-crosslinked hydrogels of CH and (poly)acrylic acid (Lee et al., 1999). The extracted kinetic constants are summarized as a function of a) DXS and b) GP content (see SI, Table S3). It can be observed that increasing the DXS concentration led to an increase of the kinetic rate constant regardless of the pH. Nevertheless, the increase in the rate constant was more pronounced at pH 7.4 than at pH 2.0. This is probably due to CH deprotonation at higher pH than the pKa of CH (approx. 6.5) that leads to weaker electrostatic interactions with the anionic DXS, and thus a more flexible porous structure capable of swelling faster and to a larger extent. On the other hand, increasing the GP concentration led to a decrease in the kinetic rate constant at pH 7.4 while the behaviour at low pH was not trivial. A very similar trend was found in a related system; Katime et al. reported an increase in the kinetic rate constants with dimethylaminoethyl acrylate methyl chloride quaternary salt (Q9) while such kinetic constants decreased with the crosslinker concentration for poly(acrylic acid-coQ9)-based hydrogels (Katime, 2010).

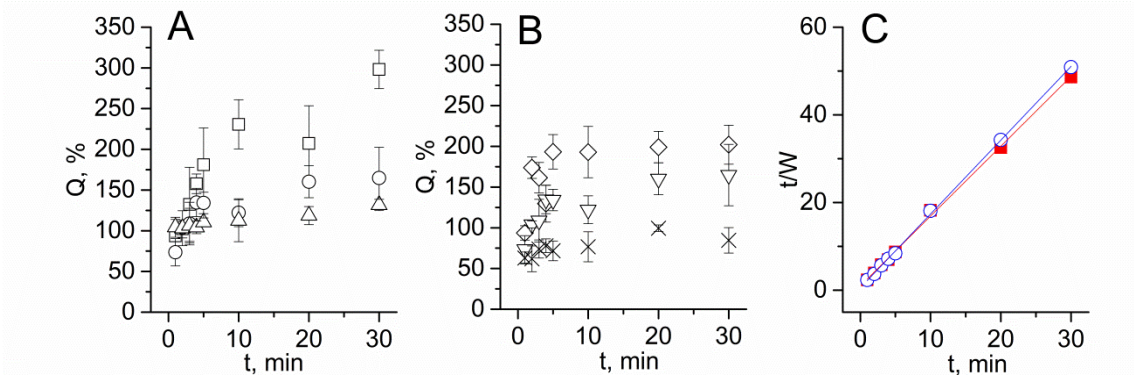

Figure 4. Swelling isotherms of hydrogels at pH 2.0 for compositions: A) 1.5 wt % CH and 0.1 wt % GP with varied DXS (squares: 0 wt%, circles: 1 wt %, and triangle: 1.25 wt %), B) 1.5 wt % CH and 1 wt % DXS with varied GP (diamonds: 0.05 wt%, inverse triangles: 0.1 wt %, and crosses: 0.15 wt %). C) Data and fits to Eq. 4 for hydrogels composed of 1.5 wt% CH, 1 wt% DXS and 0.1 wt% GP using Eq. 3 at pH 2.0 (red) and pH 7.4 (blue). Error bars represent the standard deviation from triplicate experiments.

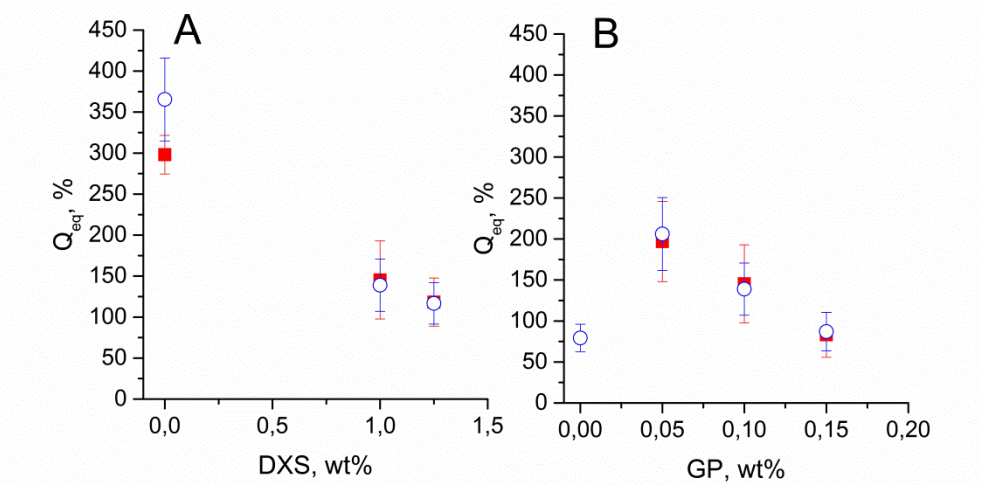

Figure 5. Equilibrium swelling percentage (Q_{eq},%) as a function of A) DXS concentration, and B) GP concentration at pH 2.0 (red) and 7.4 (black). The hydrogels in A were prepared with fixed CH (1.5 wt %) and GP (0.1 wt %) concentrations while hydrogels in B were prepared with fixed CH (1.5 wt %) and DXS (1 wt %) concentrations. Error bars represent the standard deviation from triplicate experiments.

3.4 Morphology of hydrogels

The microstructure of chemical hydrogels was investigated by SEM imaging in order to determine the effect of DXS, CH, and GP contents on the hydrogel morphology. The chemical system without DXS (Figure 6A) showed a highly porous structure with smooth surfaces. When DXS was progressively added (Figure 6B, C), the average size of the pores seemed to decrease, and the surfaces became rougher (see SI, Figure S4, for a higher magnification). Likewise, the degree of reticulation (smaller pores) and roughness of the surfaces increased with the GP concentration (Figure 6D, B, E). When the CH amount was increased, the same pore structure was observed, although the reticulation degree was lower since the CH/GP ratio was higher (see Figure 6C, F) Therefore, the proper combination of CH, DXS, and GP creates a more structured gel with a stronger network (higher reticulation and smaller pores), which is remarkably different from the morphology of the physical hydrogels or chemically crosslinked CH without DXS.

As discussed earlier, a possible use for the crosslinked hydrogels of CH and DXS is as carriers for probiotic delivery, and therefore the structure of crosslinked beads formed by the dropwise method was compared with the bulk hydrogels for the same composition (Figure 7). Essentially, the same microstructure and porosity were observed for both bulk and dropwise hydrogel beads.

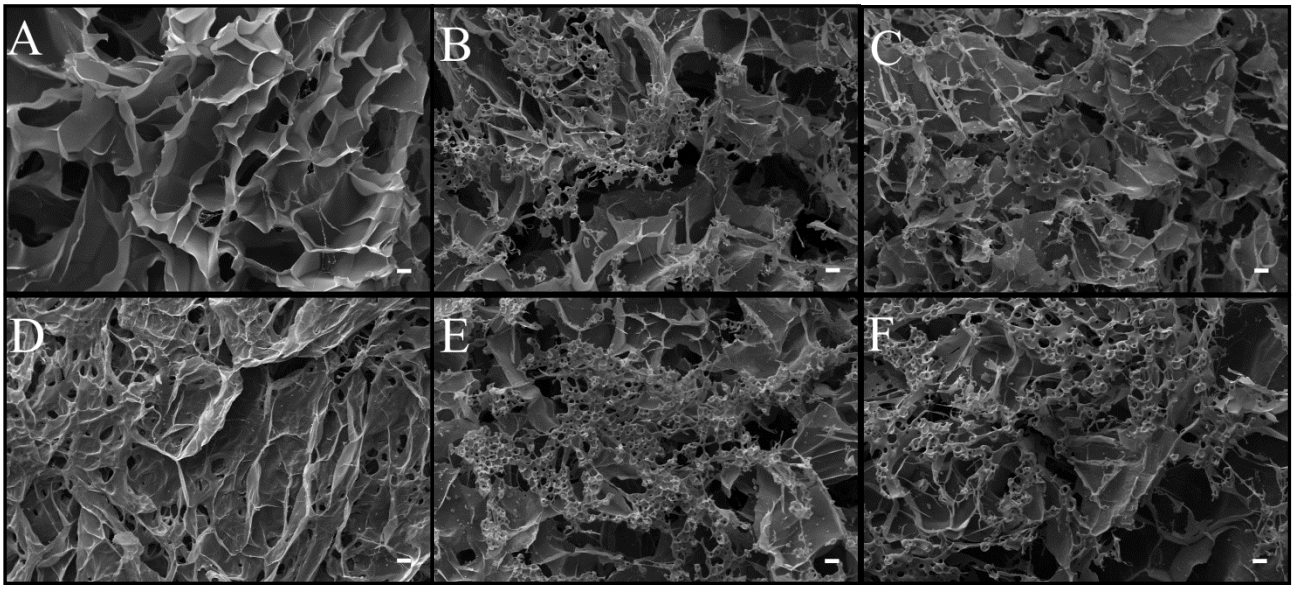

Figure 6. SEM micrographs showing the effect of DXS (A, B and C), GP (D, B and E), and CH (C and F) concentrations on the morphology of hydrogels. The composition of hydrogels in the images are as follows: A) 1.5 wt% CH, 0.1 wt% GP, B) 1.5 wt% CH, 1 wt% DXS, 0.1 wt% GP, C) 1.5 wt% CH, 1.25 wt% DXS, 0.1 wt% GP, D) 1.5 wt% CH, 1 wt% DXS, E) 1.5 wt% CH, 1 wt% DXS, 0.15 wt% GP, and F) 2.1 wt% CH, 1.25 wt% DXS, 0.1 wt% GP. The scale bar represents 20 µm.

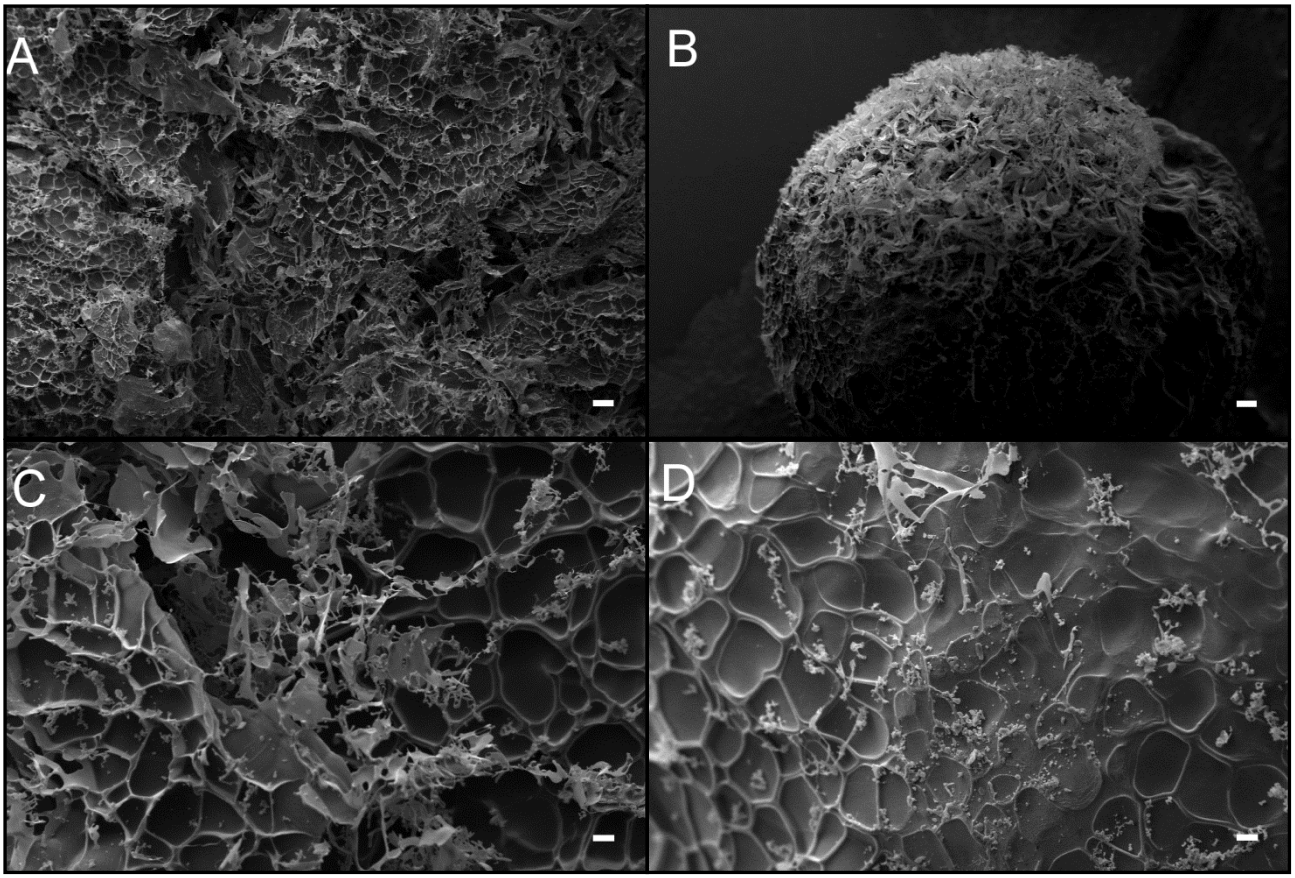

Figure 7. SEM micrographs of a bulk hydrogel (A and C) and a macro-bead (B and D) with the composition of 3 wt % CH, 2 wt % DXS and 0.1 wt % GP. The scale bars represent 100 µm (top), and 20 µm (bottom).

3.5 Cell viability and culturability

L. acidophilus (LA5) was the chosen model bacteria to be incorporated into the most promising physical and chemical hydrogels. The goal was to show the ability of the cells to divide and form offspring after interacting with different hydrogel matrices. The LA5 cell culturability was tested on solid agar surfaces and compared with the native free cells. The number of viable native cells was 8.2 ± 0.9 log CFU/mL. Figure 8A shows approx. 2.1 log CFU/mL and approx. 3.6 log CFU/mL decrease for the cells entrapped in the physical and chemical hydrogels, respectively, when compared to the number of viable native bacteria. A qualitative assessment of the viability was also performed using a live/dead staining kit (Figure 8). In Figure 8B, approx. 70-80 % of cells seem to be alive (green) after incorporation into the physical gel. This is in good agreement

with the plate counting results. The reason behind the decrease in the number of viable cells due to entrapment in hydrogels might be in part due to the hydrogel composition (if it is not neutralized, CH can display antimicrobial properties against some strains) or in part due to the rather low pH of the hydrogel (approx. 4.4). Additionally, the cell counting might be underestimated since some unreleased cells may have remained trapped in the hydrogel matrix (a small gel fraction remained as residue in the stomacher bag).

In the case of the chemical systems, the number of viable cells was less (4.6 ± 0.7 log cfu/mL) than the number of viable native cells. However, a significant amount of gel residue remained in the stomacher bag after homogenization in this case. Since this residue was not accessible, it could not be plated and counted (Figure 8C). Moreover, at least approx. 50 % of the cells in residue were estimated to be alive using live/dead viability kit in this case. Hence, bacterial cells might be viable, but not culturable. Finally, it is possible, however, that the chemical hydrogels could be further degraded in the gastrointestinal tract due to enzymatic action of gastrointestinal bacterial enzymes (Kean & Thanou, 2010).

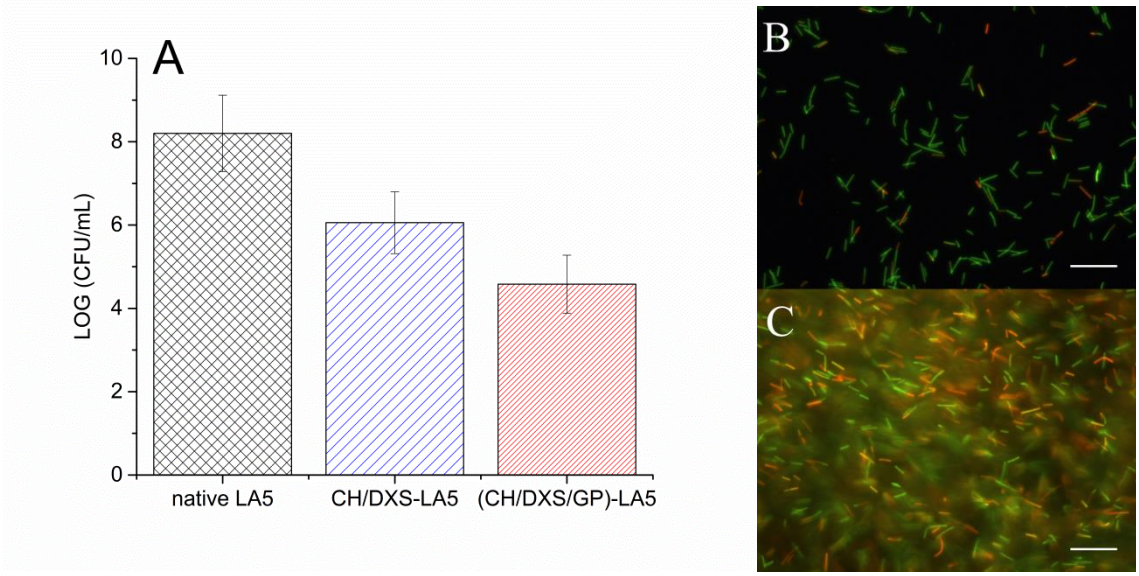

Figure 8. Viability of *L. acidophilus* (LA5) in physical hydrogel (1.5 wt % CH, 1 wt % DXS) and GP crosslinked hydrogel (1.5 wt% CH, 1wt% DXS, 0.1 wt% GP): A) plate counting results, B) microscopy image showing the live and dead cells released from a physical hydrogel and C) microscopy image showing the residue of the chemical gel exposed to live/dead staining viability kit. The scale bar represents 20 µm.

4 Conclusions

In this work, physical and GP crosslinked hydrogels of CH and DXS were developed and characterized as a potential delivery system material for probiotic bacteria encapsulation targeted the gastrointestinal tract. Physical and chemical hydrogel formulations were identified with a general non-Newtonian shear thinning and gel-like behaviour regardless of DXS, CH, and GP concentrations. An optimum CH / DXS ratio was determined (approx. 1:1) where the rheological properties were maximized independently of the pH and temperature. However, the chemical hydrogels (crosslinked with GP) were more robust and stiffer than the related physical hydrogels. The swelling of the chemical hydrogels was found to be strongly dependent on DXS and GP concentrations, not influenced by the pH of the media and obeyed a second order kinetics swelling profile. Generally, increasing either the DXS or GP led to a decrease in equilibrium swelling that was found to be in good agreement with the hydrogels microstructure (i.e. smaller pores and higher reticulation degree for samples with higher amounts of DXS and GP). Apart from the bulk hydrogels, beads were formed by the dropwise method and found to be remarkably similar to the related bulk hydrogels in terms of morphological properties. Finally, the viability and culturability tests revealed approx. 2.1 and 3.6 log CFU/mL decrease in the number of viable cells, which were incorporated in physical and chemical hydrogels, respectively. However, such values are underestimated since the qualitative viability assay (live/dead viability kit) evidenced that a considerable amount of viable cells were still entrapped in the hydrogel matrix and not released in the media used for plating. The improved mechanical properties might lead such insufficient release behavior in the case of the chemical hydrogels. It remains to be studied if the presence of specific enzymes, bile salts or other molecules can improve the release of La5 from such robust gel matrixes. Overall the systems developed are highly flexible in terms of structure and mechanical properties. By fine control of the composition and crosslinking degree it is possible to tune different features of interest such as viscoelasticity, gelling ability, swelling and microstructure/morphology. Therefore, the systems developed in this work are promising matrices for probiotic cell encapsulation and

412 delivery. In the future work, high focus will be given to the probiotic cells encapsulation in hydrogel beads
413 and the characterization of such systems in terms of viability of the encapsulated cells, their survivability in
414 simulated gastrointestinal fluid, and their release in simulated intestinal fluid.

415 **Acknowledgements**

416 The research leading to these results has received funding from the People Programme (Marie Curie
417 Actions) of the European Union's Seventh Framework Programme FP7/2007-2013/ under REA grant
418 agreement n° 606713. Bruno Medronho acknowledges the Portuguese Foundation for Science and
419 Technology (FCT) through the project PTDC/AGR-TEC/4814/2014 and researcher grant IF/01005/2014.
420 Marité Cárdenas thanks the Swedish Research Council for financial support, and acknowledges the
421 umbrella of COST actions CM1101 and MP1106.

422 ***Appendix A. Supporting Information***

423 Supplementary data associated with this article can be found, in the online version, at < insert the link >.

424 **References**

425 Altunbas, A., Lee, S. J., Rajasekaran, S. A., Schneider, J. P., & Pochan, D. J. (2011). Encapsulation of curcumin
426 in self-assembling peptide hydrogels as injectable drug delivery vehicles. *Biomaterials*, *32*(25), 5906–
427 5914. http://doi.org/10.1016/j.biomaterials.2011.04.069

428 Anitha, A., Deepagan, V. G., Divya Rani, V. V., Menon, D., Nair, S. V., & Jayakumar, R. (2011). Preparation,
429 characterization, in vitro drug release and biological studies of curcumin loaded dextran sulphate-
430 chitosan nanoparticles. *Carbohydrate Polymers*, *84*(3), 1158–1164.
431 http://doi.org/10.1016/j.carbpol.2011.01.005

432 Berger, J., Reist, M., Mayer, J. M., Felt, O., & Gurny, R. (2004). Structure and interactions in chitosan
433 hydrogels formed by complexation or aggregation for biomedical applications. *European Journal of*
434 *Pharmaceutics and Biopharmaceutics*. http://doi.org/10.1016/S0939-6411(03)00160-7

435 Bhattarai, N., Gunn, J., & Zhang, M. (2010). Chitosan-based hydrogels for controlled, localized drug delivery.
436 *Advanced Drug Delivery Reviews*. http://doi.org/10.1016/j.addr.2009.07.019

437 Butler, M. F., Ng, Y. F., & Pudney, P. D. A. (2003). Mechanism and kinetics of the crosslinking reaction
438 between biopolymers containing primary amine groups and genipin. *Journal of Polymer Science, Part*
439 *A: Polymer Chemistry*, *41*(24), 3941–3953. http://doi.org/10.1002/pola.10960

440 Delair, T. (2011). Colloidal polyelectrolyte complexes of chitosan and dextran sulfate towards versatile
441 nanocarriers of bioactive molecules. *European Journal of Pharmaceutics and Biopharmaceutics*.
442 http://doi.org/10.1016/j.ejpb.2010.12.001

443 Delmar, K., & Bianco-Peled, H. (2015). The dramatic effect of small pH changes on the properties of
444 chitosan hydrogels crosslinked with genipin. *Carbohydrate Polymers*, *127*, 28–37.
445 http://doi.org/10.1016/j.carbpol.2015.03.039

446 Dimida, S., Demitri, C., De Benedictis, V. M., Scalera, F., Gervaso, F., & Sannino, A. (2015). Genipin-cross-
447 linked chitosan-based hydrogels: Reaction kinetics and structure-related characteristics. *Journal of*
448 *Applied Polymer Science*, *132*(28), 1–8. http://doi.org/10.1002/app.42256

449 dos Santos, S., Piculell, L., Medronho, B., Miguel, M. G., & Lindman, B. (2012). Phase behavior and
450 rheological properties of DNA-cationic polysaccharide mixtures. *Journal of Colloid and Interface*
451 *Science*, *383*(1), 63–74. http://doi.org/10.1016/j.jcis.2012.06.011

452 Drury, J. L., & Mooney, D. J. (2003). Hydrogels for tissue engineering: Scaffold design variables and
453 applications. *Biomaterials*. http://doi.org/10.1016/S0142-9612(03)00340-5

454 Gupta, P., Vermani, K., & Garg, S. (2002). Hydrogels: From controlled release to pH-responsive drug
455 delivery. *Drug Discovery Today*. http://doi.org/10.1016/S1359-6446(02)02255-9

456 Hoare, T. R., & Kohane, D. S. (2008). Hydrogels in drug delivery: Progress and challenges. *Polymer*.
457 http://doi.org/10.1016/j.polymer.2008.01.027

458 Illum, L., & Davis, S. B. S. (2005). Chitosan as a Delivery System for the Transmucosal Administration of
459 Drugs. In Severian Dumitriu (Ed.), *Polysaccharides: Structural Diversity and Functional Versatility* (p. 5).
460 CRC Press.

461 Karoubi, G., Ormiston, M. L., Stewart, D. J., & Courtman, D. W. (2009). Single-cell hydrogel encapsulation for
462 enhanced survival of human marrow stromal cells. *Biomaterials*, *30*(29), 5445–5455.
463 http://doi.org/10.1016/j.biomaterials.2009.06.035

464 Katime, I. (2010). Swelling Properties of New Hydrogels Based on the Dimethyl Amino Ethyl Acrylate Methyl
465 Chloride Quaternary Salt with Acrylic Acid and 2-Methylene Butane-1,4-Dioic Acid Monomers in
466 Aqueous Solutions. *Materials Sciences and Applications*, *1*(3), 162–167.
467 http://doi.org/10.4236/msa.2010.13026

468 Kean, T., & Thanou, M. (2010). Biodegradation, biodistribution and toxicity of chitosan. *Advanced Drug*
469 *Delivery Reviews*. http://doi.org/10.1016/j.addr.2009.09.004

470 Kronberg, B., Holmberg, K., & Lindman, B. (2014). *Surface Chemistry of Surfactants and Polymers*. *Surface*
471 *Chemistry of Surfactants and Polymers*. http://doi.org/10.1002/9781118695968

472 Lee, K. Y., & Mooney, D. J. (2001). Hydrogels for tissue engineering. *Chemical Reviews*.
473 http://doi.org/10.1021/cr000108x

474 Moura, M. J., Figueiredo, M. M., & Gil, M. H. (2007). Rheological study of genipin cross-linked chitosan
475 hydrogels. *Biomacromolecules*, *8*(12), 3823–3829. http://doi.org/10.1021/bm700762w

476 Picout, D. R., & Ross-Murphy, S. B. (2003). Rheology of Biopolymer Solutions and Gels. *The Scientific World*
477 *JOURNAL*, *3*, 105–121. http://doi.org/10.1100/tsw.2003.15

478 Prabaharan, M., & Mano, J. F. (2005). Chitosan-based particles as controlled drug delivery systems. *Drug*
479 *Delivery*, *12*(1), 41–57. Retrieved from http://www.ncbi.nlm.nih.gov/pubmed/15801720

480 Ravi Kumar, M. N. . (2000). A review of chitin and chitosan applications. *Reactive and Functional Polymers*.
481 http://doi.org/10.1016/S1381-5148(00)00038-9

482 Saboktakin, M. R., Tabatabaie, R., Maharramov, A., & Ramazanov, M. A. (2010). Synthesis and
483 characterization of superparamagnetic chitosan-dextran sulfate hydrogels as nano carriers for colon-
484 specific drug delivery. *Carbohydrate Polymers*, *81*(2), 372–376.
485 http://doi.org/10.1016/j.carbpol.2010.02.034

486 Sakiyama, T., Takata, H., Kikuchi, M., & Nakanishi, K. (1999). Polyelectrolyte complex gel with high pH-
487 sensitivity prepared from dextran sulfate and chitosan. *Journal of Applied Polymer Science*, *73*(11),
488 2227–2233. http://doi.org/Doi 10.1002/(Sici)1097-4628(19990912)73:11<2227::Aid-App20>3.0.Co;2-4

489 Schott, H. (1990). Kinetics of Swelling of Polymers and Their Gels. *Journal of Pharmaceutical Sciences*, *81*(5),
490 467–470. http://doi.org/10.1002/jps.2600810516

491 Shang, J., Shao, Z., & Chen, X. (2008). Electrical behavior of a natural polyelectrolyte hydrogel:
492 Chitosan/carboxymethylcellulose hydrogel. *Biomacromolecules*, *9*(4), 1208–1213.
493 http://doi.org/10.1021/bm701204j

494 Vos, P. De, Faas, M. M., Spasojevic, M., Sikkema, J., & De Vos, P. (2010). Encapsulation for preservation of
495 functionality and targeted delivery of bioactive food components.(Report). *International Dairy*
496 *Journal*, *20*(4), 292. http://doi.org/10.1016/j.idairyj.2009.11.008

497 Vårum, K. M., & Smidsrød, O. (2005). Structure-Property Relationship in Chitosans. In Severian Dumitriu
498 (Ed.), *Structural Diversity and Functional Versatility*. CRC Press.
499 http://doi.org/10.1201/9781420030822.ch26

500 Wang, Q., & Chen, D. (2016). Synthesis and characterization of a chitosan based nanocomposite injectable
501 hydrogel. *Carbohydrate Polymers*, *136*, 1228–1237. http://doi.org/10.1016/j.carbpol.2015.10.040

502

503

504

505